Available online at www.eccomasproceedia.org
Eccomas Proceedia COMPDYN (2017) 160-177

ECCOMAS
Proceedia

COMPDYN 2017
6th ECCOMAS Thematic Conference on
Computational Methods in Structural Dynamics and Earthquake Engineering
M. Papadrakakis, M. Fragiadakis (eds.)
Rhodes Island, Greece, 15–17 June 2017

NUMERICAL SIMULATION OF THE SUSPENDED ROOF OF THE NIARCHOS CULTURAL CENTER AT ATHENS – GREECE UTILISING COMPONENT TEST RESULTS

G.C. Manos[1], V. Kourtides[2], K. Katakalos[2], L. Kotoulas [3], G. Koidis[3], K. Kyprioti[4]

[1] Professor and Director of the Lab. of Strength of Materials and Structures, Aristotle University
e-mail: gcmanos@civil.auth.gr

[2] Dr. Civil Engineer, Research Ass., Lab. of Strength of Materials and Structures, Aristotle University
e-mail: katakaloskostas@gmail.com

[3] Postgraduate student, Lab. of Strength of Materials and Structures, Aristotle University
e-mail: kotoulaslambros@gmail.com; george_florina@hotmail.com

[4] Civil Engineer, Lab. of Strength of Materials and Structures, Aristotle University
e-mail: katerina_kyprioti@hotmail.com

Keywords: Suspended Roof, Numerical Simulation, Test results of Springs and Dampers, Stavros Niarchos Cultural Center,

Abstract. *The suspended roof of the Stavros Niarchos Cultural Center (SNCC) at Athens-Greece is studied. This roof with dimensions approximately 100m x 100m is suspended by 30 suspension units composed of springs and dampers. Each suspension unit is formed by four spring, two dampers as sliding rigid core all linked with a 3-D rigid steel frame. Each suspension unit is supported on the top of a slender hollow steel column approximately 20m height, which in its turn is supported on the top rigid reinforced concrete slab of the SNCC base-isolated main building. All these columns bear the loads of the suspended roof that is a hollow reinforced concrete deck with internal webs. The characteristics of the large SNCC suspended roof are briefly presented and discussed together with the functioning of the suspension units of this roof. The effectiveness of the base isolation system for the main building of the SNCC is examined by simplified numerical models. A brief description is next presented of the experimental sequence whereby all the components of a prototype suspension unit (springs and dampers) as well as the suspension unit itself were subjected to extreme loading conditions, as required by the design loads. The measured response of the individual components of the tested suspension units formed the basis to apply numerical simulations aimed to numerically predict the observed behaviour. First, the measured performance of the individual springs and dampers forming each suspension unit is numerically simulated. Next, the measured performance of one suspension unit is also numerically simulated. Good agreement was obtained by this numerical simulation effort between measured and predicted behaviour for the tested suspension unit.*

Peer-review under responsibility of the organizing committee of COMPDYN 2017.
doi: 10.7712/120117.5414.16893

1 INTRODUCTION

This paper presents first a summary of experimental procedures that were utilized to measure at the laboratory environment the basic components of a suspension system. This system was designed and utilized in the suspended roof that was built at the top of the building complex of the "Stavros Niarchos Foundation Cultural Center" that was recently constructed in Athens, Greece, which is designated in the following as SNCC ([2], [3], [4], [5], [6]). The whole SNCC project was completed by the Impregilio-Terna joint venture. Figure 1 depicts the suspended roof on top of the main building of the SNCC, which is in-plan approximately 87m by 75m and weights approximately 480 000KN. It is based on a system of inverted pendulum bearing on the base foundation mat that is supported through numerous piles.

Figure 1. The Stavros Niarchos Cultural Center. The main building is supported on a base isolation system formed by inverted pendulum bearings. The suspended roof supported on slender hollow steel columns.

Figure 2. The base isolation system of the Stavros Niarchos Cultural Center main building formed by inverted pendulum bearings.

The base of each one of thirty slender hollow steel columns is fixed at the thick top-story slab of the SNCC main building. These steel columns are of a varying cross section and they have at their narrowest part an internal diameter equal to 340mm and a thickness equal to 32mm. They rise at a height of approximately 20m to support the suspended roof through a suspension system, which will be described in section 3. This suspension roof covers an area of

10000m2 in plan. Its weight is approximately 51000KN and is supported only on these thirty slender hollow steel columns. The main building together with the suspended roof is protected against horizontal seismic forces by the base isolation system. Moreover, the suspended roof is further protected both from the action of the vertical seismic forces as well as from the wind forces through the suspension system that provides controlled movements of the whole roof in the vertical direction. Section 2 includes a study of the effectiveness of the base isolation system through summary results from simplified numerical analyses that were performed for this purpose. Selected information on the basic components of the suspension units that form the suspensions system is presented in section 3. This is accompanied with relevant results from an experimental campaign conducted at the Laboratory of Strength of Materials and Structures of Aristotle University that had as an objective to verify the performance of one prototype suspension unit and its components. Finally, section 4 presents selected results from the numerical simulation of this prototype suspension unit and its components. It must be underlined here that all the information included here is approximate and qualitative and it does not represent the data and the methods used in the design of this important structural system.

2. NUMERICAL STUDY OF THE SNCC BASE ISOLATION SYSTEM

2.1. Simplified Numerical Analysis of the Suspended Roof and the SNCC Main Building

In this numerical study the SNCC main building is simulated as a hollow rigid box, as the objective of this study is to examine the isolation system and its interaction with the hollow steel columns and the suspended roof [2]. Three different numerical models are examined by varying the foundation conditions of the main building as well as the presence or not of diagonal stiffeners at the bays that are formed between neighbouring hollow steel columns that support the suspended roof (see figure 1). In the first case the foundation is considered as being fixed to the underlying soil. This case is numerically simulated by constraining all the nodes of the bottom slab of the rigid box simulating the main building to have zero displacements in all three directions ($u_x = u_y = u_z = 0$). In this case there are no diagonal stiffeners at the bays that are formed between neighbouring hollow steel columns that support the suspended roof. In the second model the foundation support conditions remain the same; however, this time diagonal stiffeners are added at the bays that are formed between neighbouring hollow steel columns that support the suspended roof (see figure 1). Finally, the third model includes the diagonal stiffeners; moreover, all the nodes of the bottom slab of the rigid box simulating the main building are connected with the underlying soil with linear springs, simulating in this way the base isolation system. The stiffness values of these springs in the two horizontal directions (x, y) are adjusted in such a way as the resulting two first translational eigen-modes of vibration have eigen-period values approximately equal to 2.59 sec. These were the eigen-period values of the SNCC complex with the actual base isolation system that was installed (figure 2). Initially, a frequency analysis was performed with all these three numerical models. The results are included in figure 3, 4, 5 for models 1, 2 and 3, respectively. The following observations can be made on the basis of the results of this frequency analysis. Model 1 includes the following two basic parts. a) The suspended roof together with the hollow steel columns without diagonals, which represents a very flexible system in the two horizontal directions. b) The rigid building box constrained at its base, which represents a very stiff system. The eigen-frequency analysis reveals that for the two first eigen-modes the suspended roof with the hollow steel columns vibrates along the two horizontal diagonals simultaneously in the two horizontal directions (x and y) with a relatively very large eigen-period value equal to 5.93sec (figure 3). The modal mass participation values for these two first eigen-modes represent again the vibration only of the suspended roof.

TABLE: Modal Participating Mass Ratios	Fixed foundation						
StepNum	Period	UX	UY	UZ	SumUX	SumUY	SumUZ
Unitless	Sec	Unitless	Unitless	Unitless	Unitless	Unitless	Unitless
1	5,932031	0,05893	0,04078	0	0,05893	0,04078	0
2	5,932016	0,04078	0,05893	0	0,09971	0,09971	0
3	5,59712	2,06E-11	4,94E-11	0	0,09971	0,09971	0
4	0,13791	2,34E-07	0	5,00E-20	0,09971	0,09971	5,00E-20
5	0,136256	0	0	0,1	0,09971	0,09971	0,1
6	0,121378	0	2,26E-07	0	0,09971	0,09971	0,1
7	0,059623	8,61E-20	8,22E-20	3,35E-19	0,09971	0,09971	0,1
8	0,043742	0	0	0,00006343	0,09971	0,09971	0,1
9	0,039248	1,84E-19	1,46E-19	0,00004355	0,09971	0,09971	0,1
10	0,025882	6,83E-19	1,33E-08	3,93E-18	0,09971	0,09971	0,1
11	0,025868	4,03E-09	1,25E-19	0	0,09971	0,09971	0,1
12	0,015489	8,30E-19	3,20E-11	5,78E-18	0,09971	0,09971	0,1

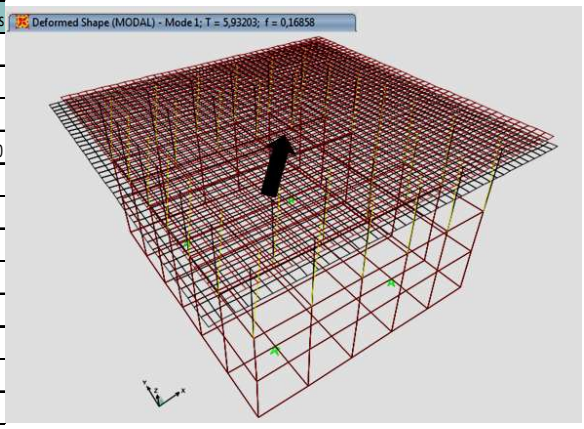

Figure 3. Eigen-periods and modal participating mass ratio values for numerical model 1.

TABLE: Modal Participating Mass Ratios –	Fixed foundation + Diagonals					
StepNum	Period	UX	UY	UZ	SumUX	SumUY
Unitless	Sec	Unitless	Unitless	Unitless	Unitless	Unitless
1	1,622769	0,09971	3,54E-13	0	0,09971	3,54E-13
2	1,544535	3,54E-13	0,09971	0	0,09971	0,09971
3	1,161845	3,89E-15	3,16E-17	0	0,09971	0,09971
4	0,135744	4,46E-08	0	8,98E-20	0,09972	0,09971
5	0,134558	0	0	0,1	0,09972	0,09971
6	0,119725	0	1,70E-08	0	0,09972	0,09971
7	0,059436	5,88E-20	1,35E-19	3,42E-19	0,09972	0,09971
8	0,043664	4,70E-20	1,01E-20	0,00006386	0,09972	0,09971
9	0,039222	5,95E-19	1,71E-19	0,00004887	0,09972	0,09971
10	0,02587	0	1,97E-08	0	0,09972	0,09971
11	0,025852	7,99E-10	0	5,27E-20	0,09972	0,09971
12	0,015487	8,74E-18	7,74E-11	1,58E-17	0,09972	0,09971

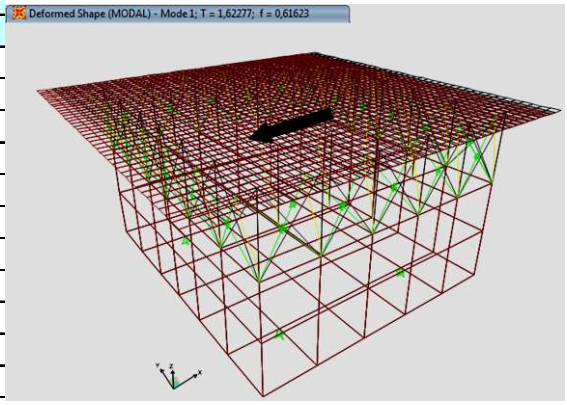

Figure 4. Eigen-periods and modal participating mass ratio values for numerical model 2.

Base isolation + Diagonals	TABLE: Modal Participating Mass Ratios						
StepNum	Period	UX	UY	UZ	SumUX	SumUY	SumUZ
Unitless	Sec	Unitless	Unitless	Unitless	Unitless	Unitless	Unitless
1	2,592443	1	1,216E-08	3,288E-20	1	1,2E-08	3,288E-20
2	2,59187	1,216E-08	1	2,979E-20	1	1	6,267E-20
3	0,732706	3,263E-20	2,963E-20	1	1	1	1
4	0,506959	0,00017	6,587E-17	0	1	1	1
5	0,480833	1,288E-17	0,0001365	0	1	1	1
6	0,375689	1,177E-17	9,242E-20	0	1	1	1
7	0,120253	3,375E-12	0	0	1	1	1
8	0,115644	0	0	6,966E-05	1	1	1
9	0,107696	0	4,188E-11	0	1	1	1
10	0,057831	0	0	0	1	1	1
11	0,042985	0	0	9,072E-10	1	1	1
12	0,038985	0	0	1,035E-09	1	1	1

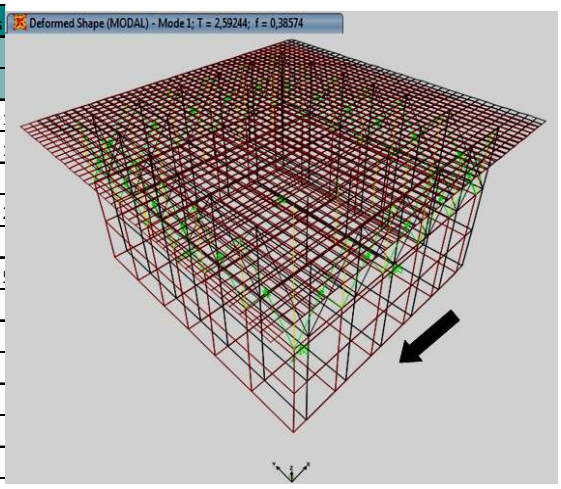

Figure 5. Eigen-periods and modal participating mass ratio values for numerical model 3.

The rigid box representing the main building does not participate in the vibration of any of the next 10 higher modes for this first model. The 5th eigen-mode of this model represents the vertical mode of vibration of the suspended roof. However, this numerical solution does not

include the actual suspension system. Thus, the eigen-period value for this vertical translation mode equal to 0.136sec results from the axial stiffness / flexibility of the slender hollow steel columns that support in this model the suspended roof. This is a fictitious case that will be altered drastically with the introduction of the suspension system, as will be discussed in what follows. The introduction of the diagonal stiffeners at the bays that are formed between neighbouring hollow steel columns that support the suspended roof (see figure 1 and 4) results in a considerable stiffening effect of the part that includes the suspended roof the hollow steel columns and the diagonal stiffeners. Despite this stiffening effect, the two first eigen-modes represent again the horizontal vibration of the suspended roof with the hollow steel columns and the diagonals along the two horizontal directions (x and y) with eigen-period values equal to 1.622 sec and 1.545sec for the x-x and y-y horizontal directions, respectively (figure 4). The modal mass participation values for these two first eigen-modes represent again the vibration only of the suspended roof. The 5^{th} mode represents again the vertical vibration of the suspended roof that remains almost unaltered. The introduction of the linear flexible 3-D links, simulating the base isolation system, resulted in three first modes whereby the suspended roof with the hollow steel columns vibrate in unison with the rigid box representing the main building. This can be seen from the values attained in this case by the modal mass participation ratio values for the first three modes that for this model is approximately 1.0. The presence of the base isolation system results in the desired increase flexibility of the total system with eigen-period values for the first two horizontal translational modes equal to 2.592sec. The vertical vibration eigen-mode becomes also more flexible than the previous two models with an eigen-period value equal to 0.733sec.

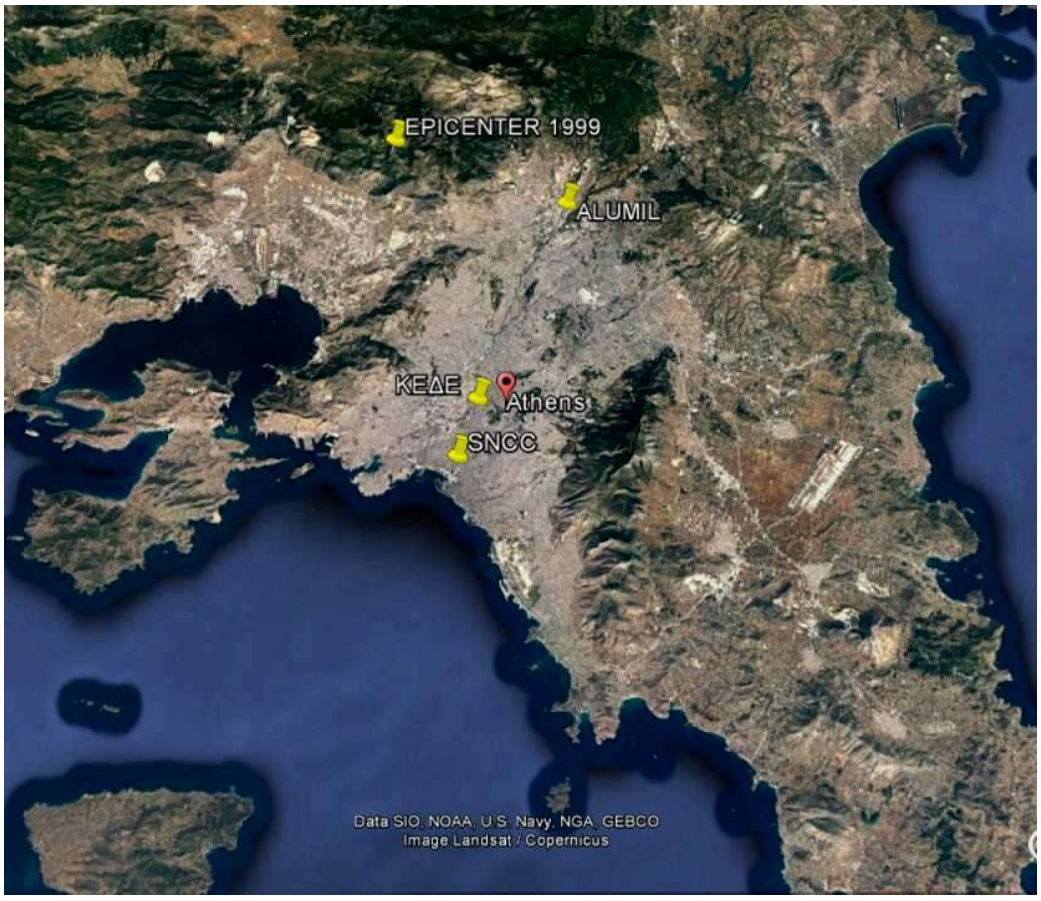

Figure 5. Map of Athens indicating the location of the epicenter of the 1999 main earthquake together with the locations of the SNCC and the site where the ground acceleration was recorded [7].

2.1.1. Approximate earthquake response of suspended roof and the SNCC main building.

The 3 models described before were subjected to a three component ground acceleration. For this purpose the ground acceleration recorded during the Athens 1999 earthquake sequence was employed. Figure 5 depicts a map of Athens, Greece indicating the location of the epicenter of the 1999 main earthquake together with the locations of the SNCC together with the location of the site where the ground acceleration was recorded (KEDE record V2, [7]). As can be seen from this figure the distance of the SNCC from the epicenter is approximately 21km whereas the distance of the SNCC from the site where the ground acceleration was recorded (KEDE) is 3.65km. The proximity of the SNCC to the site where the ground acceleration was recorded (KEDE) and its distance from the epicenter are arguments supporting the use of this recorded ground acceleration without any modifications in this preliminary analysis. The two horizontal components together with the vertical component were employed as input motion in this numerical analysis. The orientation of the axes (x and y) of the building relatively to the orientation of the horizontal components of the recorded ground acceleration was ignored at this preliminary numerical analysis. Thus, one horizontal component of this recode was applied without any modification to the x-x axis of the main building and the other to the y-y axis. The obtained absolute displacement response is shown in figures 6, 7 and 8. Figure 6 depicts the variation of the absolute horizontal displacement response at the top of the suspended roof along the direction x-x as it was obtained from model 1 (fixed base without diagonals), model 2 (fixed base with diagonals) and model 3 (base isolation with diagonals).

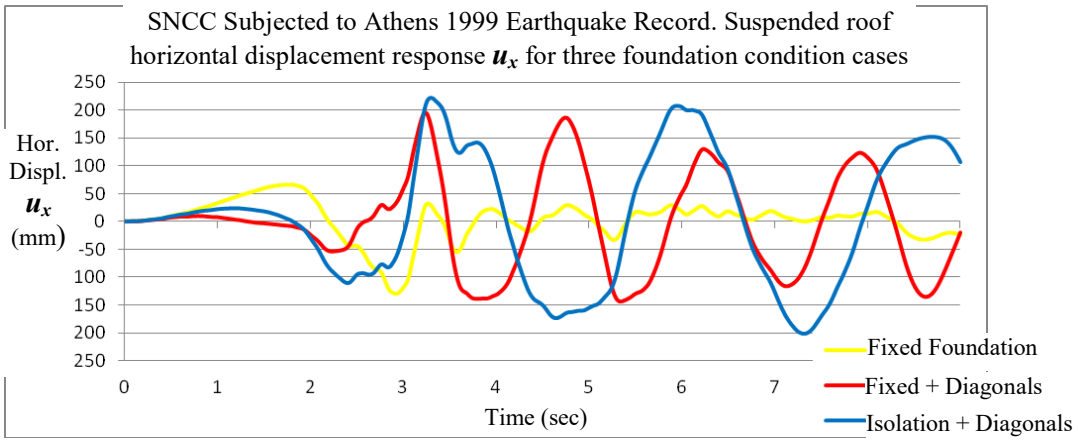

Figure 6. Absolute horizontal displacement response at the top of the suspended roof for models 1, 2 and 3.

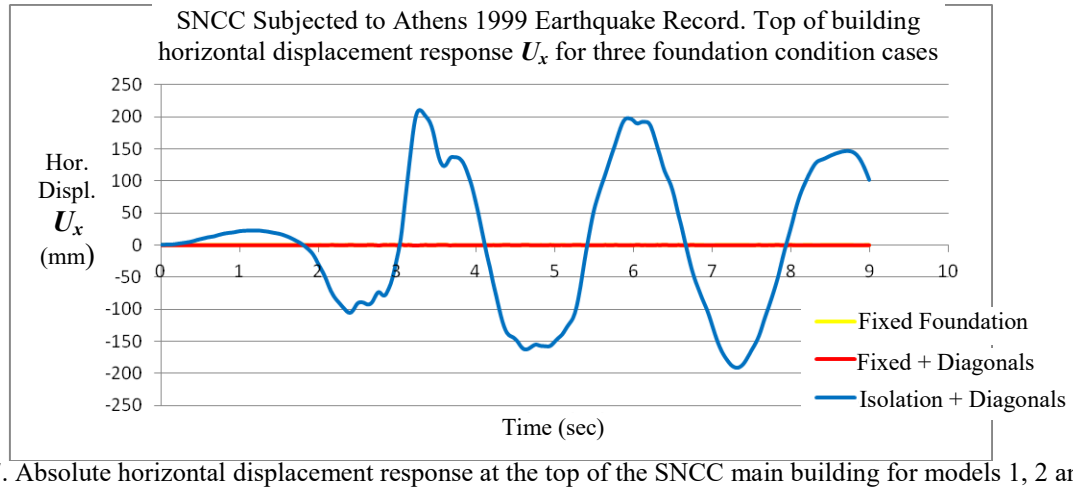

Figure 7. Absolute horizontal displacement response at the top of the SNCC main building for models 1, 2 and 3.

Figure 7 depicts the variation of the absolute horizontal displacement response at the top of the SNCC main building along the direction x-x as it was obtained from model 1 (fixed base without diagonals), model 2 (fixed base with diagonals) and model 3 (base isolation with diagonals) whereas figure 8 shows the corresponding relative horizontal displacement response between the top of the SNCC main building and the top of the suspended roof.

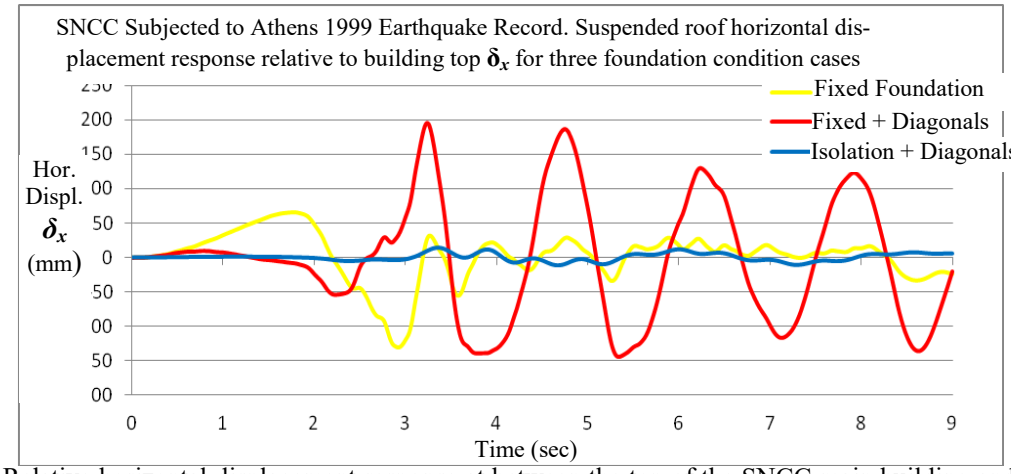

Figure 8. Relative horizontal displacement response at between the top of the SNCC main building and the suspended roof for models 1, 2 and 3.

As can be seen by comparing figures 6, 7, and 8 the base isolation is effective in minimizing the relative horizontal displacement response between the top of the building and the suspended roof. The presence of the base isolation results in amplifying the horizontal displacement response at the top of the SNCC main building which moves almost in unison with its base (figure 7). In this way both the hollow steel columns with the diagonals as well as the various connections of these columns with the suspended roof (through the suspension system) are subjected to much lesser horizontal displacement and resulting levels of stress demands than is the case when the base isolation is not in place. These observations are based on the previously described simplified numerical analyses employing the said Athens 1999 ground acceleration record. Consequently, their nature is mainly qualitative; however, it is expected to have a general validity.

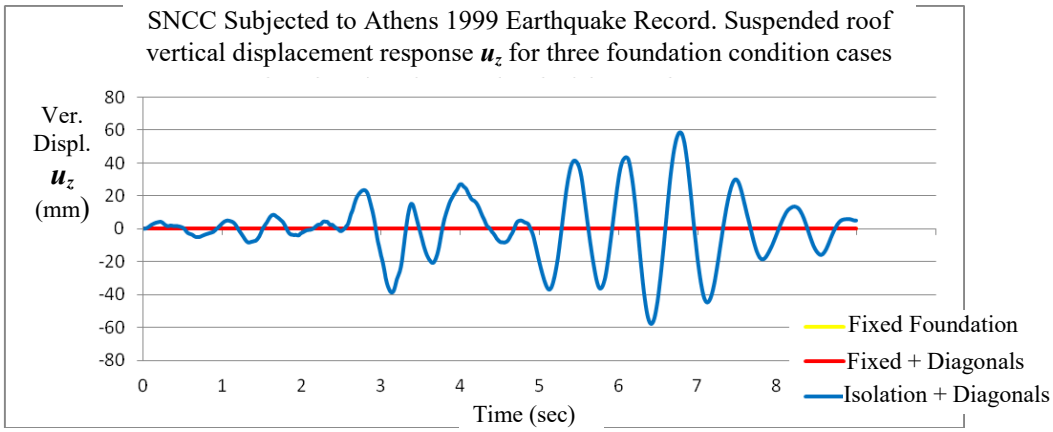

Figure 9. Absolute vertical displacement response at the top of the suspended roof for models 1, 2 and 3.

Figure 9 depicts the variation of the absolute vertical displacement response at the top of the suspended roof along the direction z-z as it was obtained from model 1 (fixed base without diagonals), model 2 (fixed base with diagonals) and model 3 (base isolation with diagonals). As can be seen, the presence of the base isolation is expected to introduce a vertical displacement response of the SNCC building to flexibility of the isolators in the vertical direction. However, the relative vertical response between the suspended roof and the top of the SNCC building is not portrayed by this analysis which presumed for all three models that the connection between the top of the hollow steel columns and that of the suspended roof is rigid. This interaction in the vertical direction is further examined when the suspension system is introduced for connecting the suspended roof with the hollow steel columns.

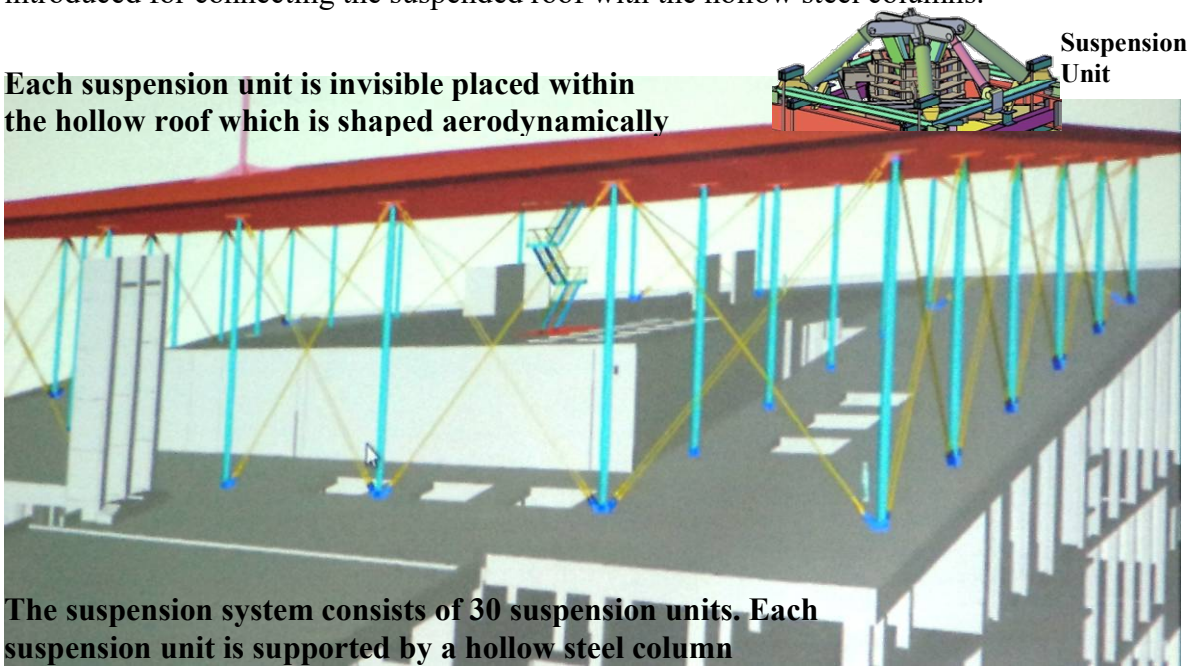

Figure 10. A sketch of the hollow suspended roof with the suspension units that are hosted within the spaces of the hollow roof.

Figure 11a. Reinforcement of the pre-cast parts of the hollow roof

Figure 11b. One corner part of the aerodynamically shaped hollow roof.

3. DESCRIPTION OF THE SUSPENSION SYSTEM

Figure 10 is a sketch of the suspended roof that covers the top of the SNCC main building being supported by thirty (30) hollow steel columns as already described. At the top of each column a suspension unit is fixes, as it is schematically shown in figure 10 ([2], [3], [4], [5], [6]). Each unit is hosted within the spacing of the aerodynamically shaped hollow roof which is made of many pre-cast parts that are lifted and assembled in situ on top of the columns be-

ing supported by a form-work. Each of these pre-cast parts was constructed with numerous small diameter reinforcing bars together with high strength ferro-cement as shown in figures 11a and 11b. The finished suspended roof of the SNCC is depicted in figure 12.

Figure 12. The finished suspended roof at the top of the SNCC main building.

3.1. Composition of each suspension unit.

Each suspension unit is formed by a 3-D polygonal steel rigid frame with dimensions in plan approximately 4m x 4m. This steel frame is depicted in figure 13 as it rests on top of the strong reaction frame of the laboratory of Strength of Materials and Structures of Aristotle University. Its external perimeter is approximately a square formed by strong steel girders that are strengthened even more at the four corners where the connection with the suspended roof is established. In the central part of the suspension unit an octagonal steel sub-frame is formed that is rigidly connected to the strong peripheral steel square frame. This octagonal frame extends both above and below the horizontal plane that is formed by the central lines of the peripheral square sub-frame steel girders. The external part of this octagonal frame can be seen in figures 13 and 14.

Figure 13. The 3-D polygonal steel rigid frame of a suspension unit. The 4 strong corners of this frame that represent the connection areas to the hollow suspended roof are also visible.

Figure 14. The rigid steel core with the sliding pads. This core slides within a polygonal rigid frame that is also visible at the center of figure 13.

In the internal sides of this octagonal steel frame sliding surfaces of cylindrical shape are rigidly attached thus forming a cylindrical surface that can house tightly a sliding core as shown in figure 14. This sliding core is also provided with special sliding parts to ensure a stable vertical sliding of the core within the octagonal steel sub-frame. The special sliding pads ensure a coefficient of friction below 2%. Figures 15 and 16 depict a typical suspension unit being assembled for testing at the laboratory of Strength of Materials and Structures of Aristotle University ([3], [4], [5]). Four springs are then placed to connect the four corners of the square peripheral rigid frame with the four top corners of the sliding core, as depicted in figure 15. Furthermore, two dampers are place to also connect the top of the sliding core with the square peripheral rigid frame. All the connections of these springs and dampers, at one end to the sliding core and at the other end to the peripheral square rigid frame, are made with cylindrical hinges having a horizontal axis. In this way the completed suspension unit is formed consisting of four springs, two dampers, a 3-D rigid steel frame. In the central part of this 3-D rigid frame a vertical cylinder is formed to house the core that is designed to slide freely in the vertical direction. The bottom part of this sliding core is rigidly connected to the top of the corresponding slender hollow steel column that is supported to the top strong slab of the SNCC main building (see figures 1, 10 and 12). Figures 13, 14, 15 and 16 depict the assembling process of all the described parts which were transported at the laboratory premises for testing. After numerous tests they were again disassembled and transported at the construction side to be hoisted to become part of the suspension roof system.

Figure 15. Four springs connecting the four top corners of the sliding core to the four corners of the 3-D square steel rigid frame of a suspension unit.

Figure 16. A damper that connects the top of the sliding core with the perimeter of the 3-D octagonal steel rigid frame of a suspension unit

In this way the roof is suspended to the sliding core and in turn to the hollow steel columns through these springs and dampers, which can be extended or contracted from an initial equilibrium condition depending on the variation of the vertical load demand that is transferred upon them from the roof. These springs are always in tension, as they have been extended from their smallest length condition to meet the demand of the dead load imposed on them when the suspended roof was gradually freed from the temporary formwork, which was supporting it during construction. This is shown in the central part of figure 17. The roof has to withstand extra vertical loads directed down-wards (e.g. snow etc.). This is shown in the left part of figure 17. In this case, the springs are further extended developing larger tensile forces than the one for the equilibrium dead load condition. Finally, the roof has to withstand vertical loads directed upwards (e.g. wind, earthquake etc.). This is again shown in the right part of

figure 17. The springs in this case are contracted developing smaller tensile forces than the ones for the equilibrium dead load condition.

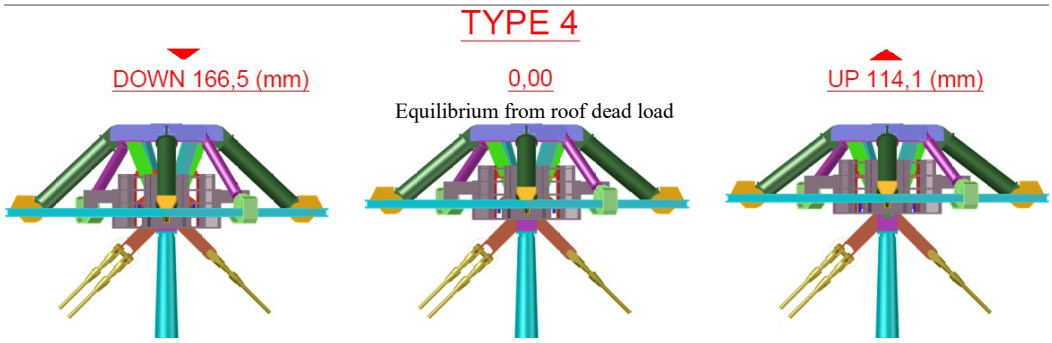

The roof has to withstand extra vertical loads directed downwards (e.g. snow etc.). The springs are further extended developing large tensile forces.

The springs are extended up to a point in order to develop the tensile forces to balance the roof dead weight. The roof moves downwards.

The roof has to withstand vertical loads directed upwards (e.g. wind, earthquake etc.) The springs are contracted. Their tensile forces are decreased accordingly.

Figure 17. The basic functioning of one suspension unit as part of the suspended roof.

During the experimental sequence the tested suspension units were supported at the four corners of the square rigid steel sub-frame constraining all the movements at these locations along the two horizontal axes (x, y) as well as the vertical axis (z). In order to replicate the function of the suspension unit that was described before the bottom part of the sliding core was connected to a vertical hydraulic jack supported by a strong reaction floor. This jack was capable to subject the sliding core at this bottom location to vertical upward forces that were sufficient to displace the sliding core (***billet***) upwards thus forcing the four springs and dampers also to be extended. In this way, the springs develop the relevant tensile forces that equilibrate the vertical load applied by the hydraulic jack. This is depicted in figure 18.

Vertical load is applied to the billet and being resisted by the equivalent extension of the springs

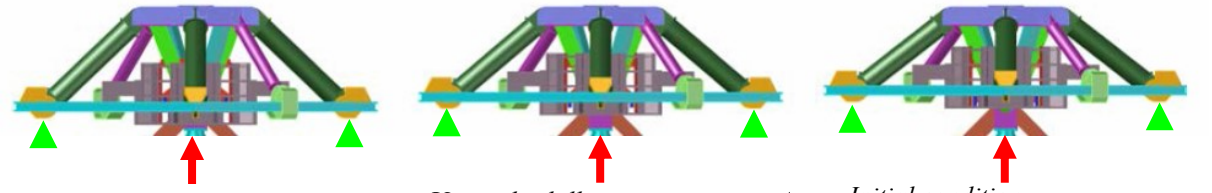

Upward billet movement of 280.6mm. The springs are fully extended. This corresponds to the maximum vertical load condition

Upward billet movement of 114.1mm. The springs are extended to a length corresponding to the roof dead weight condition

Initial condition. The springs are at their shortest length corresponding to the minimum vertical load condition

▲ *Support points of the suspension unit to the reaction frame*

Figure 18. The basic functioning of one suspension unit during the experimental sequence.

4. EXPERIMENTAL SEQUENCE

The objectives of the experimental sequence are briefly described here ([3], [4] and [5]). A first task was to test individually each one of the four springs forming a suspension unit. This was done by subjecting each individual spring to numerous tests whereby its extension covered all its prescribed working range. Details on the loading arrangement of each individual spring are included in the previously published work by Manos et al. [3]. Figure 19a depicts the fitting of one of these springs at the loading frame whereas figure 19b shows the measured axial load-displacement response of one of these springs as it was measured at Aristotle University together with discrete measurements provided by the manufacturer. As can be seen the load-displacement response of this spring exhibits a slightly non-linear behaviour that is also accompanied by a hysteretic loop.

Figure 19a. Spring being fitted at the loading frame

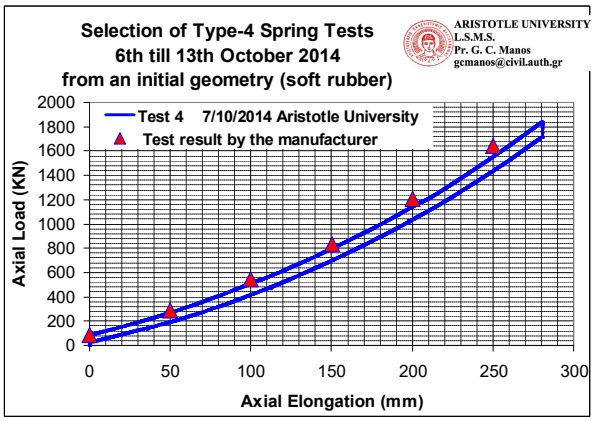

Figure 19b. Axial load-displacement response of a spring

Next, each one of the employed dampers was also tested. These dampers had to undergo also numerous tests with main variable the velocity of the applied imposed axial displacement. This was achieved by employing a variety of imposed sinusoidal or triangular displacement time histories with variable amplitude and frequency.

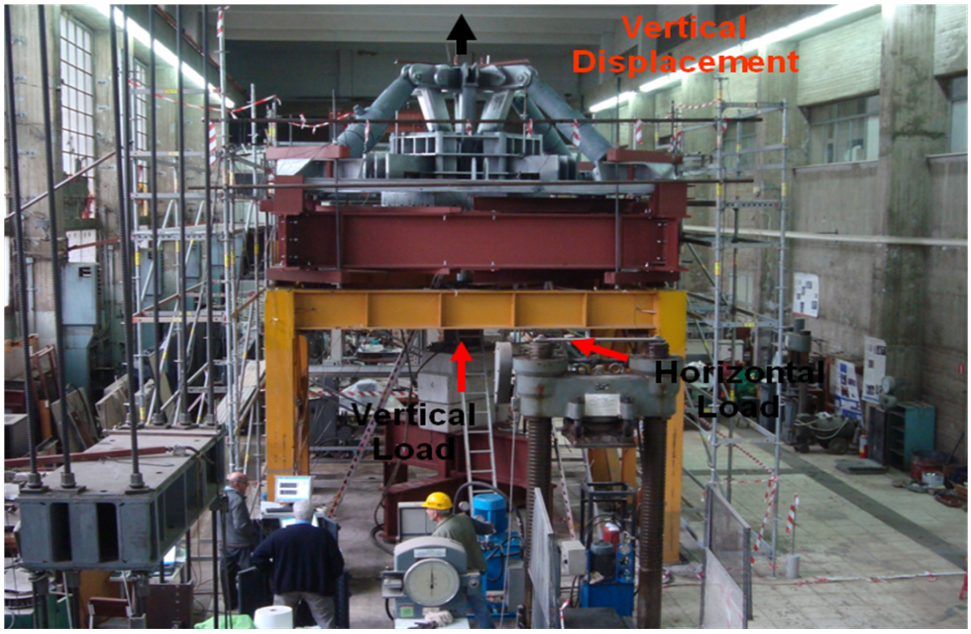

Figure 20. The suspension device CHA Type-4 being supported at the strong reaction frame (brown and yellow colour) together with the hydraulic jack installed in a way to apply the required vertical load at the center of the billet (sliding core).

After the performance of each spring and damper was measured individually the suspension unit was assembled and it was subjected to the previously described loading sequence (see figures 18 and 20). With this laboratory loading arrangement (figures 18 and 20) the basic loading functions of the prototype suspension device in-situ (section 3) was simulated in laboratory conditions. Two suspension devices were tried; the first on that was designated as CHA Type-4 and the 2nd one that was designated as CHA Type-1. A considerable number of tests were performed for each suspension device varying the following parameters:

a1) The inclusion during testing in the device of the relevant two dampers. Thus the same tests were repeated with and without the two dampers.

b1) The simultaneous application at the low part of the billet a certain level of horizontal load, as shown in figure 20, in order to check the performance of the device when apart from the upward and downward displacement each device was subjected to a certain level of bending moment with a tendency to create a rotation φ1 of the billet relative to the surrounding hollow steel cylinder, as is shown in figure 21. This horizontal load was applied through an additional horizontal hydraulic jack at the lowest part of the billet, as shown in figure 21. For each tests the level of horizontal load was kept constant whereas the level of vertical load and vertical displacement of the billet varied from the minimum to the maximum levels (section 3). For every vertical load variation two different levels of horizontal load (H) was checked, either horizontal load equal to zero (H=0) or horizontal load equal to H=400KN for CHA Type-4 or H=280KN for CHA Type-2. This combination of vertical and horizontal forces has been applied for all structural formations (with or without dampers).

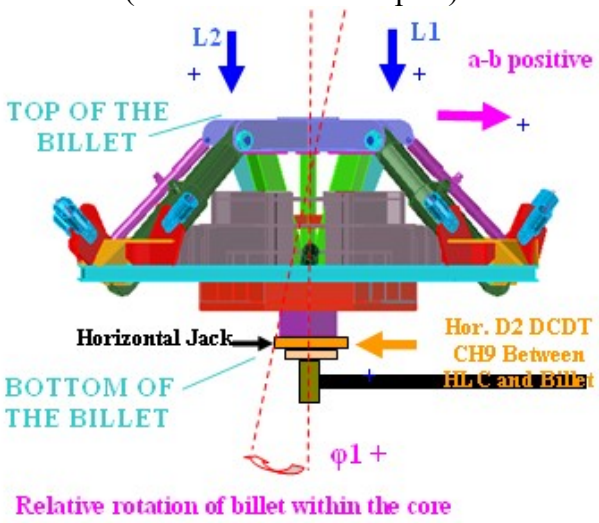

Figure 21. Imposed rotation of the billet relative to the hollow steel cylinder of the horizontal frame through the application of the appropriate horizontal load.

c1) The vertical load (V) / vertical billet (δ_v) displacement that was applied through the vertical hydraulic jack was applied in two different ways. First, this vertical displacement was applied in a continuous non-stop manner from the minimum to the maximum level and then after a brief stop back to the minimum level. Secondly, the vertical load (V) / vertical billet (δ_v) displacement was applied in 20mm vertical displacement intervals from the minimum to the maximum level and then after a brief stop back to the minimum level again in 20mm vertical displacement intervals.

The above parametric variation in the way the vertical load (V) / vertical billet (δ_v) displacement was applied was tried in combination with the variation of the previous two parameters; that is with or without the two dampers and with or without the horizontal H. This parametric variation was done together with the requirement to check the repeatability of the observed performance for each combination by performing at least three identical tests for each combination. This resulted in a large number of tests and in a similar large number of corresponding measurements.

4.1. Instrumentation scheme and test results

In order to measure the response of the various parts of the tested prototype suspension device specimens at the laboratory a number of load and displacement sensors were attached on the specimens that were continuously recording during testing. The vertical and the horizontal load were measured at the location where they were applied at the bottom of the billet level (figure 21). Moreover, the vertical displacement of the sliding billet relatively to the surrounding hollow cylinder (and the horizontal steel frame) was measured with three vertical displacement sensors that were fixed at the upper billet level (figure 3). The rotation of the billet relatively to the hollow steel cylinder was measured in two independent ways. First, by the differences recorded in the measurement of the vertical displacement of the billet relatively to the surrounding hollow steel cylinder as these vertical displacement sensors were fixed in three different places at the periphery of the billet's upper level. Secondly, by installing horizontal displacement transducers that measured the horizontal displacement of the billet relative to the hollow steel cylinder in two perpendicular directions at both the bottom billet level as well as at the top billet level, the rotational response of the billet was found. Apart from this instrumentation that is very essential to understand and describe the important behavioral characteristics of the performance of the CHA specimens additional instrumentation was also provided in order to check the proper operation of the experimental facility especially that of the supporting reaction frame. For this purpose, additional displacement transducers were installed in order to ensure that the CHA specimens were practically fixed at their four supports; in addition, strain gauges were also installed on the pre-stressing bars in order to get the proper warning in the case of an accidental overstress of these pre-stressing rods in transferring the forces that developed on the suspension device during testing.

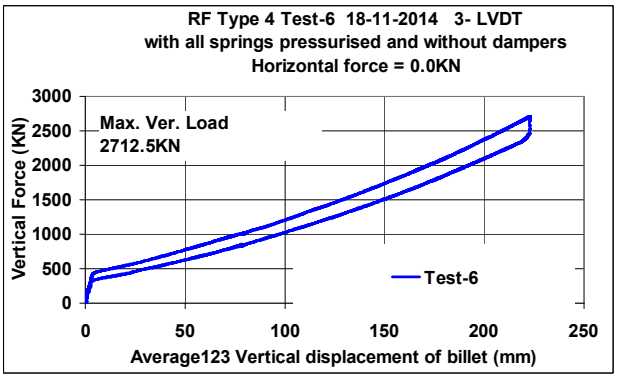

Figure 22a. Axial load-displacement response of suspension unit Type-4 without dampers. Only vertical load is applied.

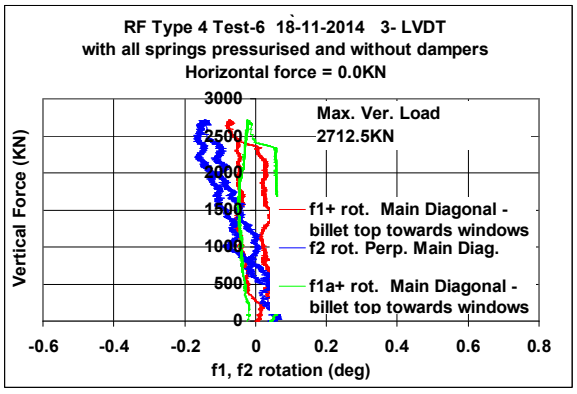

Figure 22b. Axial load- rotation of the billet response of suspension unit Type-4 without dampers. Only vertical load is applied.

Figure 22a depicts the axial load-displacement response of suspension unit Type-4 without dampers when it is subjected to only vertical load. The vertical load was applied from an ini-

tial condition with the springs being fully contracted and the billet being in its lowest possible location. The vertical load was applied upwards and was accompanied by an upward sliding vertical displacement of the billet. This movement of the billet, as explained in section three caused a corresponding extension of the four springs and a consequent tension that equilibrated the applied vertical load. The maximum vertical load that was applied during the test shown in figure 22a on the suspension unit was equal to 2712.5KN and it was accompanied by an upward vertical movement of the sliding billet having a maximum values equal to 222.83mm. When this maximum displacement/load was reached it was sustained for sometime and the load was slowly released allowing the suspension unit to return to its original unloaded condition. Each load/unload cycle at this stage of testing was performed with a rate ranging from 0.7mm/sec till 2.0mm/sec. As can be seen in figure 22a the load-displacement response of this suspension unit exhibits again a slightly non-linear behaviour that is also accompanied by a hysteretic loop as it was already pointed out based on the measured behaviour of the individual springs. Figure 22b shows the rotational response of the billet when it is sliding within the cylindrical sliding surface of the 3-D rigid steel frame of the suspension unit (see section 3), when this unit is subjected to only vertical load during testing. Based on the measured rotational response of the billet during the application of the vertical loading in its full range it was demonstrated that the movement of the billet is almost vertical without any significant rotation that could inhibit its smooth sliding.

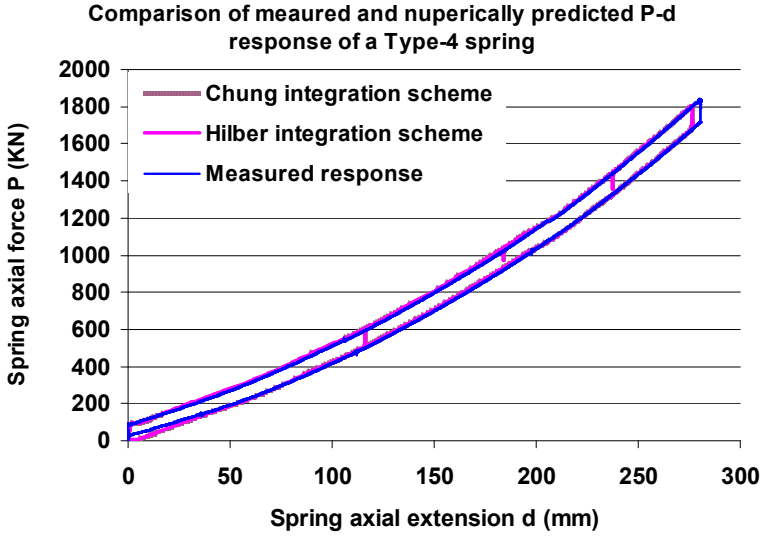

Figure 23. Measured and predicted axial load-displacement response of a spring

5. NUMERICAL SIMULATION OF THE OBSERVED PERFORMANCE

In this section summary results will be presented from a numerical simulation of the behaviour of the suspension unit. Initially this numerical simulation will be confined on the behaviour of the individual spring. Based on the success of this individual spring numerical simulation the behaviour of the suspension unit will be numerically simulated next ([2], [5]).

5.1. Numerical simulation of the measured performance for an individual spring.

The numerical simulation of the observed spring behaviour (see figure 19b) is attempted employing a multi-linear elastic spring combined with two 3-D non-linear springs which follow a plasticity constitutive low defined by the user. The non-linear analysis is a step-by-step time

history analysis that employed two different time integration schemes that are included in the used software package. The obtained results are depicted in figure 23 whereby the predicted spring axial load versus axial displacement response is compared with the corresponding measured behaviour. As can be seen in this figure good agreement can be obtained between observed and predicted spring response. Moreover, the results obtained from the two different integration schemes are very similar.

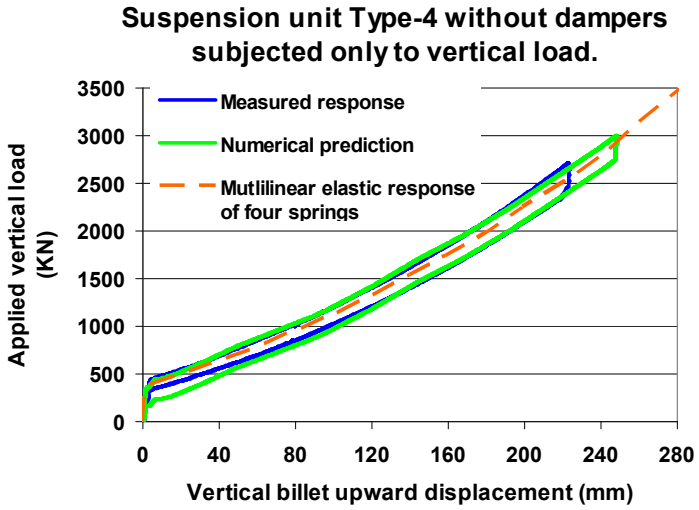

Figure 24a. Measured and predicted axial load-displacement response of suspension unit Type-4.

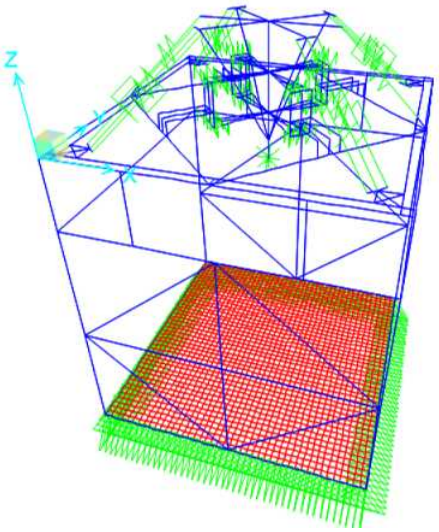

Figure 24b. Numerical model of suspension unit Type-4

5.2. Numerical simulation of the measured performance for suspension unit Type-4.

Following the successful numerical simulation of the individual Type-4 spring the numerical simulation effort was extended to the Type 4 suspension unit. The numerical model reproduced exactly the geometry of all the parts of this suspension unit as well as of the reaction frame and strong floor that supported this unit at the laboratory and was used to apply the vertical load. This is shown in figure 24b. Each of the four springs was numerically simulated in exactly the same way that was described in section 5.1. Moreover, the numerical model included a simulation of the octagonal rigid frame at the central part of the suspension unit as well as the rigid core. Contact link elements were utilized to numerically reproduce the sliding of the billet relatively to the internal cylindrical surface of the octagonal frame.
Because the displacement of the springs due to the vertical sliding movement of the billet was not only axial an adjustment of the constitutive law for the multi-linear spring was introduced by multiplying the corresponding multi-linear law of the individual spring by 1.4. As can be seen in figure 24a good agreement can be seen between the numerically predicted and the measured response for a suspension unit Type-4 without dampers subjected only to vertical load. In an alternative numerical simulation the option of non-linear analysis with large displacements was applied [1]. The numerical simulation was again for the same suspension unit Type-4 without dampers and only when vertical load was applied. The obtained response is depicted in figure 25. As can be seen with the utilization of the large displacement option that is available in this option resulted in a suspension unit response prediction through the non-linear time-history analysis that is in good agreement with the measured response without the need of any adjustment, as described before.

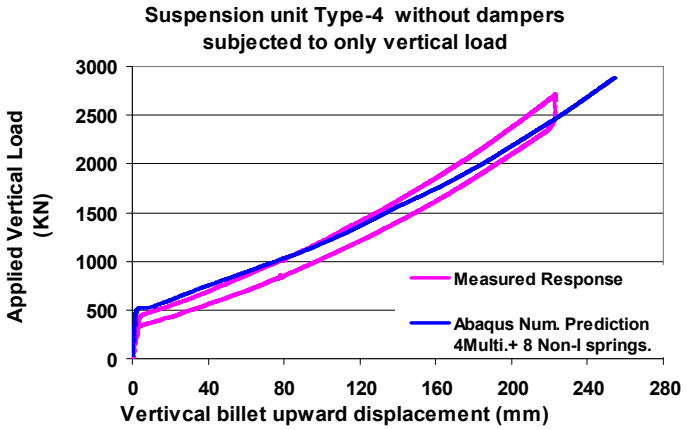

Figure 25. Measured and predicted axial load-displacement response of suspension unit Type-4 utilizing the large displacements option [1].

6. CONCLUSIONS

- The characteristics of the large suspension roof of the Stavros Niarchos Cultural Center are briefly presented and discussed together with the functioning of the suspension units that form the suspension system of this roof
- The effectiveness of base isolation system for the main building of the cultural center is examined by simplified numerical models. It is demonstrated that the base isolation is effective in minimizing the relative horizontal displacement response between the top of the building and the suspended roof. The presence of the base isolation results in amplifying the horizontal displacement response at the top of the SNCC main building which move almost in unison with its base. In this way both the hollow steel columns with the diagonals as well as the various connections of these columns with the suspended roof (through the suspension system) are subjected to much lesser horizontal displacement and resulting levels of stress demands than is the case when the base isolation is not in place. These observations are based on simplified numerical analyses employing the Athens 1996 ground acceleration record. Consequently, their nature is mainly qualitative; however, it is expected to have a general validity.
- A brief description is next presented of the extensive experimental sequence whereby all the components of a prototype suspension unit (springs and dampers) as well as the suspension unit itself were subjected to extreme loading conditions, as required by the design loads. It was shown that the load-displacement response of this suspension unit exhibits non-linear behaviour that is also accompanied by a hysteretic loop similar to the measured behaviour of the individual springs. Moreover, based on the measured rotational response of the sliding core of this suspension unit (billet) during the application of the vertical loading in its full range it was demonstrated that the movement of this (billet) is almost vertical without any significant rotation that could inhibit its smooth sliding.
- The measured response of the individual components of the tested suspension units formed the basis to apply numerical simulations aimed to numerically predict the observed behaviour. This was tried first for the springs and then for the suspension unit. Good agreement could be obtained between the numerically predicted and the measured response for a suspension unit Type-4 without dampers subjected only to vertical load. When the option of large displacement non-linear time history analysis was utilized it was not necessary to adjust the properties of the multi-linear links employed to simulate the behaviour of the

individual springs. Otherwise, an adjustment of the relevant constitutive law was necessary using a multiplier equal to 1.4.

- All the finding of the experimental sequence were employed to make necessary corrections of the construction process in order to safeguard the desired performance of such an important and structural project.

ACKNOWLEDGEMENTS

The consultations with Emeritus Professor George Penelis, Dr. Gregory Penelis, Dr. Kostas Antoniadis and Dr. Kostas Paschalidis as well as with the representatives of Expedition Engineering and the Impregilio-Terna joint venture are gratefully acknowledged. The consultations and financial support of MAGEBA S.A of Switzerland that provided all the springs and dampers, which formed the tested suspension devices, and in particular Mr. Achilleas Athanasiou is thankfully noted. The effort of the personnel of the Laboratory of Strength of Materials and Structures and in particular of Thomas Koukouftopoulos is also thankfully acknowledged. Finally, the encouragement and support of the Stavros Niarchos Foundation is also acknowledged.

- To the memory of Ray W. Clough, Professor Emeritus of the University of California, at Berkeley, U.S.A.

REFERENCES

[1] Hibbitt, Karlsson, Sorensen. Inc. ABAQUS user's manual volumes I–V and ABAQUS CAE manual. Version 6.10.1. Pawtucket, USA; 2010.

[2] Kyprioti K. "Study of the dynamic and earthquake response of a suspended roof", Postgraduate thesis, Dept. Civil Engineering, Aristotle University, 2016 (in Greek).

[3] Manos G.C., Kourtides V., Katakalos K., Kotoulas L., Nalmpantidou A., "Study of the Loading Arrangement for the Stiffness Tests of the Column Head Assembly and its Springs Utilized at the Niarchos Cultural Center at Athens – Greece", COMPDYN 2015, Greece, 25–27 May 2015.

[4] Manos G.C. "Final Report on the testing sequence of the SNFCC Column Head Assembly Type-4 and Type-1 specimens together with the performance of individual springs and dampers", July 2015.

[5] Manos G.C. et al. "Study" Proceedings of the Hellenic Conference on Concrete Structures, Thessaloniki, Nov. 2016 (in Greek).

[6] Penelis G., Penelis G., Paschalidis K., Papanikolaou V. and Paraskevopoulos E., "T-H Dynamic and Non-linear Static Analysis for the PV Canopy of the New Athens Opera House", 2nd European Conf. on Earthquake Engineering and Seismology, Istanbul, August 25-29, 2014.

[7] "Athens, Greece 1999 Strong motion data", Institute of Earthquake Engineering and Engineering Seismology data base, ITSAK, Greece.